Title

Mussel Coating Protein-Derived Complex Coacervates Mitigate Frictional Surface Damage.

Journal

ACS Biomaterials Science & Engineering, 1(11)

ISSN

2373-9878

Authors

Miller, Dusty

Das, Saurabh

Huang, Kuo-Ying

et al.

Publication Date

2015-11-09

DOI

10.1021/acsbiomaterials.5b00252

Peer reviewed

ACS Biomaterials SCIENCE & ENGINEERING

Article

pubs.acs.org/journal/abseba

Mussel Coating Protein-Derived Complex Coacervates Mitigate Frictional Surface Damage

Dusty Rose Miller,[†] Saurabh Das,[‡] Kuo-Ying Huang,[§] Songi Han,[§] Jacob N. Israelachvili,[‡] and J. Herbert Waite*[,§]

[†]Biomolecular Science and Engineering Program, University of California, Santa Barbara, California 93106-9611, United States

[‡]Department of Chemical Engineering, University of California, Santa Barbara, California 93106-5080, United States

[§]Department of Chemistry and Biochemistry, University of California, Santa Barbara, California 93106-9625, United States

ABSTRACT: The role of friction in the functional performance of biomaterial interfaces is widely reckoned to be critical and complicated but poorly understood. To better understand friction forces, we investigated the natural adaptation of the holdfast or byssus of mussels that live in high-energy surf habitats. As the outermost covering of the byssus, the cuticle deserves particular attention for its adaptations to frictional wear under shear. In this study, we coacervated one of three variants of a key cuticular component, mussel foot protein 1, mfp-1 [(1) *Mytilus californianus* mcfp-1, (2) rmfp-1, and (3) rmfp-1-Dopa], with hyaluronic acid (HA) and investigated the wear protection capabilities of these coacervates to surfaces (mica) during shear. Native mcfp-1/HA coacervates had an intermediate coefficient of friction (μ ~0.3) but conferred excellent wear protection to mica with no damage from applied loads, $F_{\perp}$, as high as 300 mN (pressure, P, > 2 MPa). Recombinant rmfp-1/HA coacervates exhibited a comparable coefficient of friction (μ ~0.3); however, wear protection was significantly inferior (damage at $F_{\perp}$ > 60 mN) compared with that of native protein coacervates. Wear protection of rmfp-1/HA coacervates increased 5-fold upon addition of the surface adhesive group 3,4-dihydroxyphenylalanine, (Dopa). We propose a Dopa-dependent wear protection mechanism to explain the differences in wear protection between coacervates. Our results reveal a significant untapped potential for coacervates in applications that require adhesion, lubrication, and wear protection. These applications include artificial joints, contact lenses, dental sealants, and hair and skin conditioners.

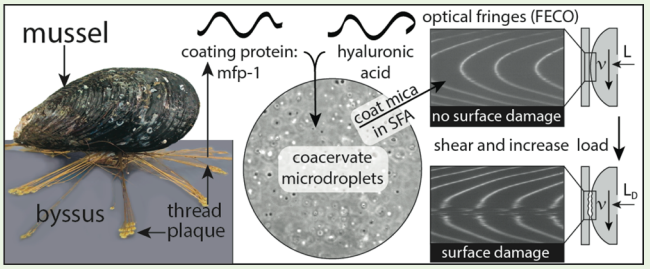

KEYWORDS: *biomimetic, adhesion, wear protection, interface, Mytilus californianus foot protein 1, mcfp-1, hyaluronic acid, HA*

1. INTRODUCTION

California mussels (*Mytilus californianus*) live sedentary lives along wind- and wave-swept shores where waves (with velocities up to 25 m/sec) impose unrelenting lift and drag forces that threaten mussel dislodgement.[1] Mussels resist dislodgement via an adaptive, fibrous holdfast known as the byssus (Figure 1a). Byssal threads mitigate wave impact by dissipating up to 72% of the applied wave energy, thereby mediating sessile attachment.[2] Friction is key to mediating energy dissipation; yet understanding the underlying phenomena relating to energy dissipation in friction is a long-standing and challenging issue in physical science.[3] Given the vast applications of friction, lubrication, and wear protection, there is much interest in understanding and implementing relevant design concepts from nature. California mussels are an excellent model system for understanding adaptive mechanisms of energy dissipation and friction under shear. A deeper understanding of the mussel byssal attachment system continues to inspire new materials including adhesives, coatings, and hydrogels.

Although the majority of the literature focuses on adhesive forces, frictional forces arguably contribute more to holdfast performance. For example, when a single attached byssal thread with a plaque is pulled normal to the surface (e.g., lift), detachment resistance is largely adhesive, whereas when pulled at low angles to the surface (e.g., drag), detachment resistance is an order of magnitude greater due to the added contribution of friction.[4] Mussels have adaptations at multiple length scales (nm−cm) that utilize friction to dissipate energy.[5,6] These adaptations include, but are not limited to, the radial distribution of anchoring threads,[7,8] the spatulate morphology of plaques,[9] the stiff to compliant thread gradient,[10] the reversible plastic deformation of threads in tension,[2,11] and an outer protective coating called the cuticle composed of hard spherical granules (diam 0.2 to 1 μm) dispersed in a continuous compliant matrix.[12] Frictional forces, however, are highly context-dependent and can also lead to stress concentration, damage, and catastrophic failure.[13]

As the outermost covering of the byssus, the cuticle deserves particular attention for its adaptations against three types of

Received: June 10, 2015
Accepted: September 14, 2015
Published: October 8, 2015

DOI: 10.1021/acsbiomaterials.5b00252
ACS Biomater. Sci. Eng. 2015, 1, 1121−1128

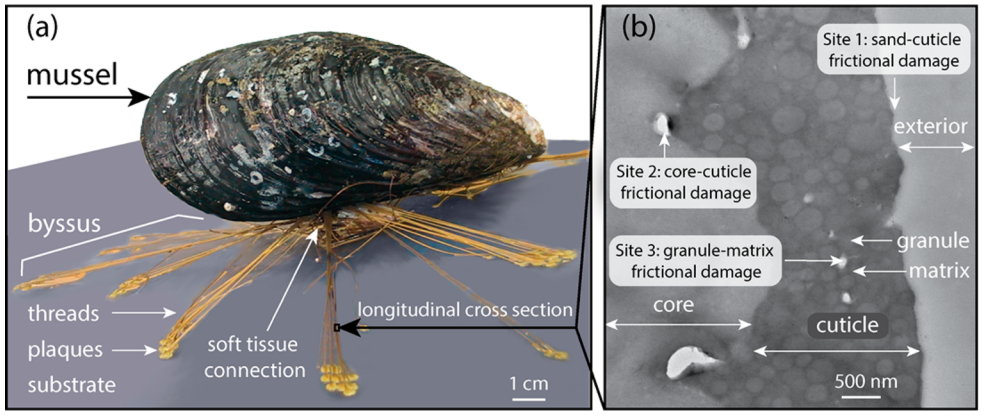

Figure 1. *M. californianus* byssus. (a) Mussel byssus mediates modulus mismatch between the hard substrate and soft tissue in the high-energy intertidal zone, where mussels are threatened with dislodgement by lift, drag, and abrasion. (b) Transmission electron micrograph of a longitudinal cross-section [zoom-in of the boxed area in panel a] of the thread core and cuticle. As the outermost covering of the byssus, the cuticle serves as a vanguard of resistance to three major types of frictionally induced damage. Site 1: sand-cuticle frictional damage. Site 2: core-cuticle frictional damage. Site 3: granule-matrix frictional damage.

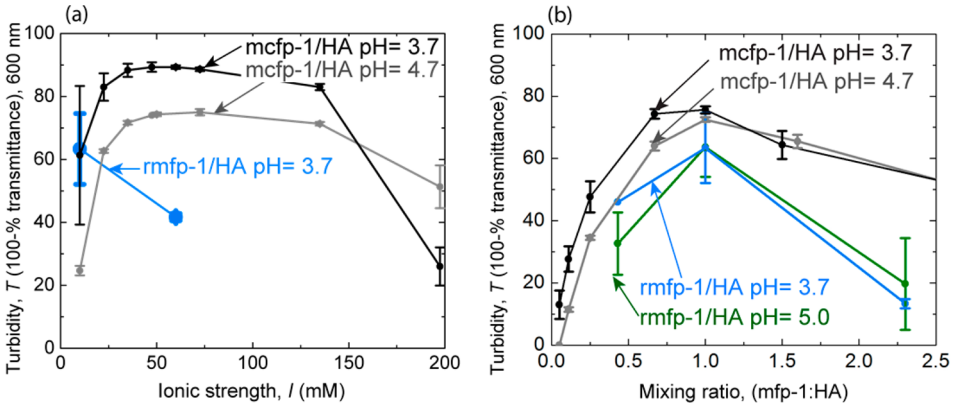

Figure 2. Coacervation dependence on ionic strength, *I*, and polycation to polyanion mixing ratio. Turbidity via transmittance at 600 nm wavelength indicates complex coacervate formation. (a) Ionic strength dependence was measured at mixing ratios with maximum turbidity (1:1 wt/wt mixing ratio of mfp-1/HA). (b) Mixing ratio dependence was measured at an ionic strength with maximum turbidity (60 mM NaCl, 10 mM acetate buffer for mcfp-1/HA, and 10 mM acetate buffer for rmfp-1/HA coacervates). Turbidity was measured 1 min post-mixing the polycation and polyanion, at room temperature, in 10 mM acetic acid/sodium acetate, and at the indicated pH. Data are presented as the mean and standard deviation, $n = 3$.

frictional damage: (1) abrasion of the exterior surface by sand, (2) interface deformation between the harder cuticle (E_i 2 GPa) and the softer collagenous core (E_i 0.4 GPa), and (3) deformation of the matrix sliding between the granules[14] (Figure 1b). The cuticle is remarkable for its ability to avoid catastrophic failure through microcracking[14] and reversible deformation.[2,10] In *M. californianus*, the cuticle is stiff (E_i 2 GPa) yet extensibile (120%), making it one of the most energy tolerant materials known.[13,15]

From a molecular perspective, the cuticle granules are preformed by condensation of mussel foot protein-1 (mcfp-1) through extensive Dopa-Fe^{3+}-complexation in the accessory gland.[16] mcfp-1 is a highly modified, positively charged, intrinsically unstructured protein with 72 decapeptide repeats of the consensus sequence PKISYP**P*TY*K [where P* is hydroxyproline, P** is dihydroxyproline, and Y* is dihydroxyphenylalanine (Dopa)].[17,18] Upon material secretion, the cuticle granules are coated by the matrix, producing the dispersion evident in Figure 1b. The matrix consists of mcfp-1 and an acidic, chymotrypsin-labile, Ca^{2+}-binding protein.[13,19] These two polyelectrolytes in the matrix are thought to be delivered as a complex coacervate.

Coacervation is an emerging theme in protein processing as used by mussels, sandcastle worms, and caddisfly larvae to concentrate, separate, and deposit polyelectrolytes underwater.[20,21] Complex coacervation relies on Coulombically driven interactions between oppositely charged groups on distinct polyelectrolytes (polycations and polyanions) to bring about phase separation, whereby the polyelectrolytes become concentrated in a dense phase that settles on and coats surfaces underwater.[22] In the mussel byssus, coacervates are proposed to both deliver adhesive proteins (mfp-3s) and form the cuticle matrix.

As a tough and energy-dissipative material, the cuticle provides an excellent model of frictional wear protection. We therefore created cuticle matrix mimics and used the surface forces apparatus (SFA) to investigate friction and surface damage mitigation. We made matrix mimics via complex coacervation of mcfp-1 (or its recombinant homologue) and hyaluronic acid (HA), a readily available biopolymer that is acidic, binds calcium, and has a mass that is well matched to that of mfp-1.[23,24] Coacervated mcfp-1/HA from *M. californianus* robustly mitigated surface damage to mica, far surpassing (>4 fold) that of coacervated recombinant homologues and native mcfp-1/HA coacervates at uneven

DOI: 10.1021/acsbiomaterials.5b00252
ACS Biomater. Sci. Eng. 2015, 1, 1121−1128

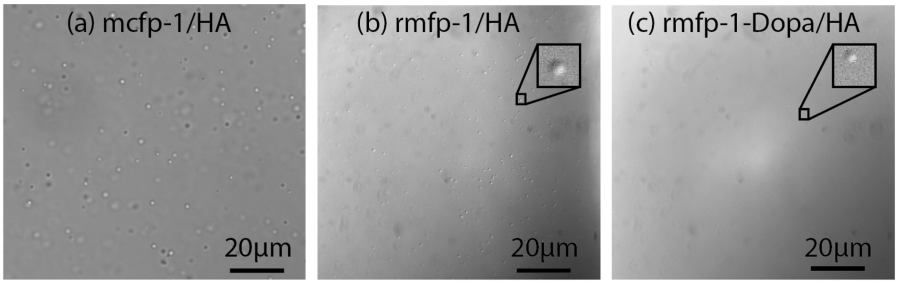

Figure 3. Bright field images of spherical coacervate microdroplets. (a) mcfp-1/HA (10 mM acetate buffer, pH 3.7, 60 mM NaCl, and 0.3 mg/mL), (b) rmfp-1/HA (10 mM acetate buffer, pH 3.7, and 0.3 mg/mL), and (c) rmfp-1-Dopa/HA (10 mM acetate buffer, pH 3.7, and 0.3 mg/mL). Images were taken 5−10 min post-mixing. Darker and lighter spheres are out-of-plane and in-plane droplets, respectively.

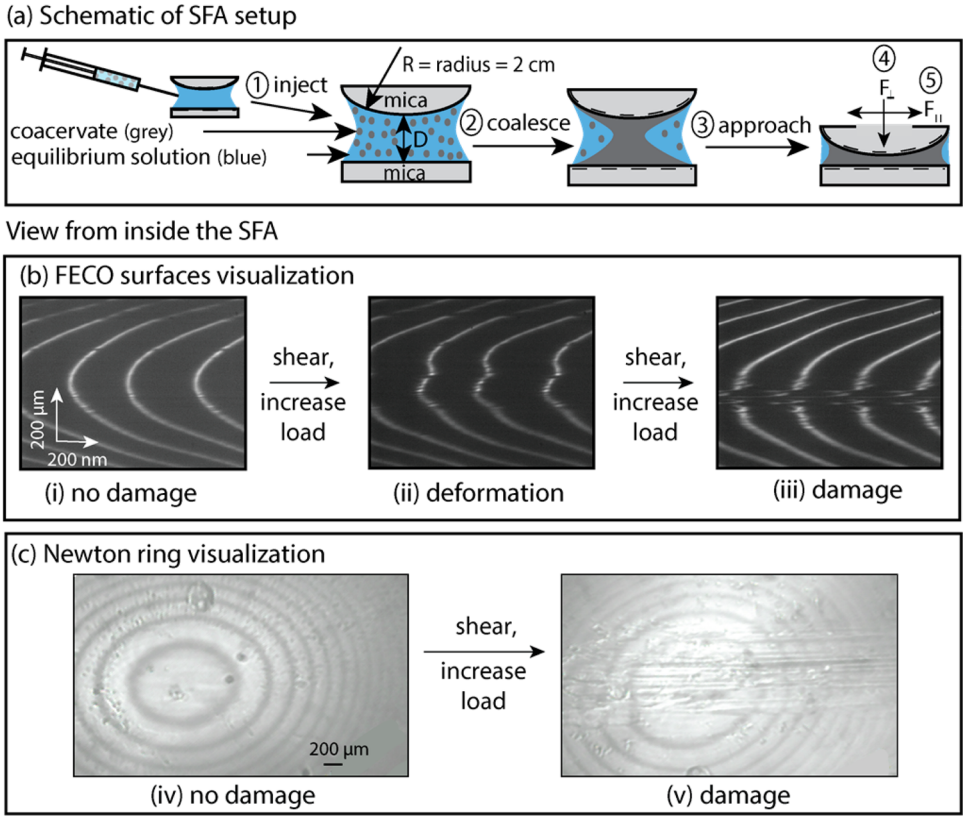

Figure 4. Experimental SFA setup and visualization of surface damage. (a) In this schematic, (1) coacervate was injected between two mica surfaces, (2) then coalesced, settled on, and coated the mica surfaces, before (3) the surface approach, for (4) normal and (5) shear measurements (see Materials and Methods, section 5.5). Representative (b) FECO and (c) Newton rings used to determine surface damage. Uninterrupted (i) FECO and (iv) Newton rings at the start of the experiment indicated a pristine surface, (ii) distorted fringes indicated the onset of wear, and (iii) FECO and (v) Newton ring interruptions indicated severe wear.

mixing ratios. During compressive shear, surface damage mitigation was independent of the coefficient of friction but instead depended critically on surface adhesive groups (Dopa) and coacervation conditions. We propose that a surface adhesive layer protects the surface from damage by shifting the shear slip-plane away from the surface and into the bulk.[25] This exceptional damage mitigation expands the role of complex coacervates in mussel byssus from fluidic intermediates in material processing to a functional structure with energy-dissipative and protective properties.

2. RESULTS

2.1. Complex Coacervation of Native mcfp-1 and rmfp-1 with HA. We measured coacervate formation via solution turbidity and transmittance at a wavelength of 600 nm. We observed that mfp-1/HA coacervation was dependent on the polycation to polyanion mixing ratio, pH, and ionic strength, I. At high ionic strengths, long-range electrostatic interactions are typically shielded (Debye length <1 nm). However, in mcfp-1/HA coacervates transient, solvent-mediated Coulombic interactions, responsible for coacervate formation and stability, persisted at high ionic strengths (mcfp-1/HA: I = 40−140 mM, Figure 2a). For mcfp-1/HA coacervates, turbidity plateaus at a maximum ranging from 40 to 140 mM in ionic strength (Figure 2a), whereas rmfp-1/HA coacervates exhibit maximum turbidity at 10 mM ionic strength, the lowest ionic strength tested. We measured turbidity at different mixing ratios at an ionic strength with maximum turbidity (10 mM for rmfp-1/HA coacervates and 60 mM for mcfp-1/HA coacervates). Turbidity measurements at

DOI: 10.1021/acsbiomaterials.5b00252
ACS Biomater. Sci. Eng. 2015, 1, 1121−1128

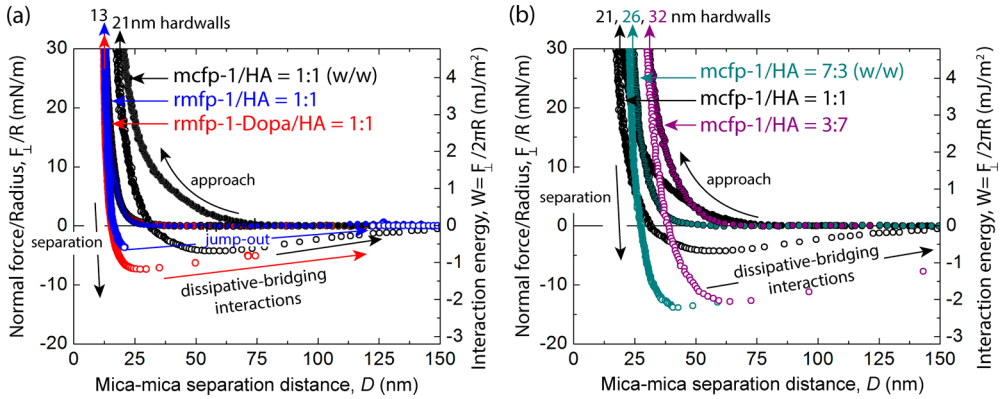

Figure 5. Representative normal force, $F_\perp$ (normalized by the radius of curvature R) as a function of mica−mica separation distance, D. Comparison of (a) native- to recombinant-based coacervate adhesion/cohesion profiles: mcfp-1/HA 1:1 ratio (black), rmfp-1/HA (blue), and rmfp-1-Dopa/HA (red). Comparison of (b) mcfp-1/HA coacervate adhesion/cohesion profiles at varying mixing ratios: mcfp-1/HA 7:3 ratio (teal), mcfp-1/HA 1:1 ratio (black), and mcfp-1/HA 3:7 ratio (purple). The hardwall is defined as the minimum separation observed under compression for the given normal force measurement. Forces measured on approach are indicated by solid circles and on separation by open circles. Jump-out during separation indicates mechanical instability, whereas dissipative-bridging interactions indicate continuous interaction during separation.

varying mixing ratios peak at a 1:1 weight-to-weight mixing ratio, which corresponds to a 0.71:1 polycation-to-polyanion charge ratio for both mcfp-1/HA and rmfp-1/HA coacervates (Figure 2b and Materials and Methods, section 5.4). We performed rheology and tribology measurements at an ionic strength with maximum turbidity (10 mM for rmfp-1/HA coacervates and 60 mM for mcfp-1/HA coacervates) and at both optimal (1:1) mixing ratios and suboptimal (7:3, and 3:7) mixing ratios with respect to coacervate yield.

Turbidity measures a metastable (time dependent) process. Upon mixing the polycation and polyanion, the turbidity increased due to microdroplet formation (time = t = 0−0.25 min), after which turbidity was metastable (t = 0.25−20 min). Finally, turbidity decreased as microdroplets coalesced with other microdroplets, settled on, and coated the cuvette surface (t = 20 min−2 d). Therefore, we measured turbidity 1 min post-mixing, well within this metastable regime.

While transmittance measurements are unable to distinguish precipitates from coacervates, we confirmed a liquid coacervate phase by observing spherical, dispersed microdroplets (Figure 3).[26] Furthermore, we confirmed a single, continuous coacervate phase by observing a uniform refractive index between the two mica surfaces, creating smooth Fringes of Equal Chromatic Order (FECO) in the Surface Forces Apparatus (SFA) (Figure 4).[24]

2.2. Energy Dissipation, E_d, and Interfacial Energy, γ_{eff}, of mcfp-1/HA and rmfp-1/HA Coacervates. We measured normal forces, $F_\perp$, at varying distances, D, between two mica surfaces in the SFA with physisorbed coacervates in the presence of bulk solution (schematic shown in Figure 4a). We then calculated the adhesive/cohesion forces, F_{ad}, using the equation $F_{ad} = F_\perp/R$ where R is the radius of surface curvature. Smooth, continuous pull-outs in the F_{ad} vs D plots imply dissipative-bridging interactions. Integration of these pull-out curves quantifies the dissipative energy, E_d.[27] We only observed dissipative-bridging interactions in coacervates containing Dopa. mcfp-1/HA coacervates demonstrated dissipative-bridging interactions at all mixing ratios (mcfp-1/HA 1:1 ratio, E_d = 32 ± 15 mJ/m^2; 7:3 ratio, 58 ± 53 mJ/m^2; 3:7 ratio, 42 ± 12 mJ/m^2, Figure 5a). We observed dissipative-bridging interactions (E_d = 63 ± 18 mJ/m^2) with rmfp-1-Dopa/HA coacervates, whereas sharp jump-outs (no dissipative-bridging interactions) were observed between surfaces with rmfp-1/HA coacervates lacking Dopa (Figure 5b).

The ability of a coacervate to coat a surface depends critically on its adhesion/cohesion energy, E_{ad}, and the interfacial energy, γ_{eff}. We calculated the interfacial energy using the minimum F_{ad} (maximum force required to separate the two surfaces) and the equation $\gamma_{eff} = F_{ad}/3\pi R$.[28] The interfacial energy of all coacervates tested was low [7:3 mcfp-1/HA; γ_{eff} = 0.61 ± 0.41 mJ/m^2, 3:7 mcfp-1/HA; γ_{eff} = 0.43 ± 0.37 mJ/m^2, rmfp-1/HA; γ_{eff} = 0.34 ± 0.11 mJ/m^2, and rmfp-1-Dopa/HA; γ_{eff} = 0.72 ± 0.17 mJ/m^2 (Figure 5a and b)]. Moreover, mcfp-1/HA coacervates at a 1:1 mixing ratio had the lowest interfacial energy (γ_{eff} = 0.28 ± 0.08 mJ/m^2) of all the coacervates tested.

2.3. Tribology and Rheology of mcfp-1/HA and rmfp-1/HA Coacervates. We used the SFA to measure the lateral forces, $F_\parallel$, to determine the tribological and rheological properties of our coacervates. Here, wear protection is as the maximum load, F_D, that coacervate-coated mica surfaces could withstand before splitting of the FECO idicated shear-induced damage to the mica surface (Figure 4b). Neither mcfp-1 nor HA in uncoacervated solution protected the surfaces from damage any more than the buffer alone (surfaces were damaged ∼10 mN).[27,29] mcfp-1/HA (1:1) coacervates protected mica from damage, even at the maximum applied load, F_D of 300 mN (corresponding to a pressure >2 MPa, Figure 6). mcfp-1/HA coacervates with uneven mixing ratios failed to protect the mica surface at 4-fold lower loads (7:3 ratio, F_D = 73 ± 53 mN; 3:7 ratio, F_D = 53 ± 18 mN). rmfp-1-Dopa/HA protected surfaces from wear under 5-fold higher loads (F_D = 57 ± 18 mN) than recombinant coacervates without Dopa (F_D = 11 ± 3 mN, Figure 6). All coacervate systems exhibited a similar coefficient of friction (μ ∼ 0.3, Figure 6, inset) during shear, save one: 7:3 mcfp-1/HA (μ = 0.5 ± 0.07). To investigate reversibility, we increased the normal force which increased the lateral force, $F_\parallel$, linearly, and both forces followed the same trajectory upon decreasing loads, even if the load was increased past the point of damage.

3. DISCUSSION

Mussel tenacity in the high-energy intertidal zone depends critically on and is defined by the vagaries of friction. Friction mediates plaque adhesion but also leads to abrasive damage to

DOI: 10.1021/acsbiomaterials.5b00252
ACS Biomater. Sci. Eng. 2015, 1, 1121−1128

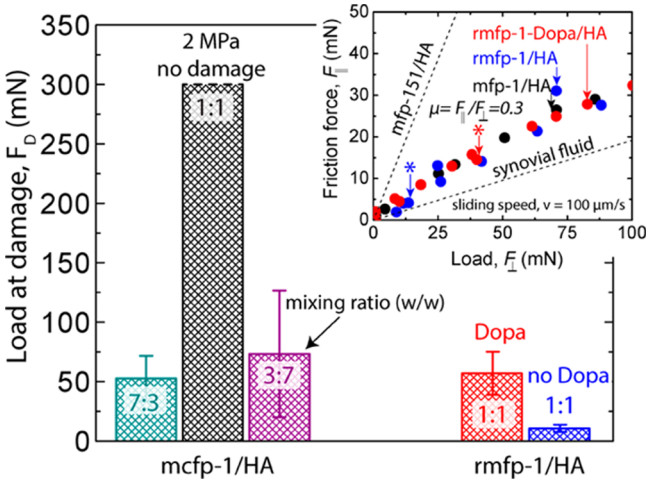

Figure 6. Mfp-1/HA coacervates' coefficient of friction (inset) and damage mitigation, as demonstrated by the magnitude of load (F_D) before shear-induced damage. Five different mfp-1/HA coacervate systems are compared: mcfp-1/HA 7:3 ratio (teal), 1:1 ratio (black), and 3:7 ratio (purple) compared to rmfp-1-Dopa/HA (red) and rmfp-1/HA (blue) ratios. Data are the means and standard deviations for n = 3−4. Inset: Friction force ($F_{\parallel}$) vs normal load ($F_{\perp}$) for native and recombinant coacervates. For comparison, the coefficient of friction of rmfp-151/HA coacervates (μ = 1.3)[24] and synovial fluid (μ = 0.15)[28] from previous works have been included. * Indicates where damage occurred (see inset).

the byssus and catastrophic failure. Mussel byssus attachment tenacity in the high-energy intertidal zone depends critically on friction;[30,31] yet, friction can also result in abrasive damage to the byssus and catastrophic failure. The mussel byssus has adapted a hard cuticular coating to resist frictional damage from sand particles and debris. However, having a hard cuticle to confer wear resistance raises concerns about other damage modes such as frictional damage within the cuticle between the softer cuticle matrix and harder cuticle granules (Figure 1b).

In this research, we explored frictional damage mitigation by shearing mfp-1/HA complex coacervates between two mica surfaces. Cuticle matrix-inspired coacervates were composed of HA and one of three mfp-1 variants: (1) *M. californianus* mcfp-1, (2) rmfp-1, and (3) rmfp-1-Dopa. We designed mfp-1/HA matrix-inspired blends to be injectable and deliverable in a concentrated form underwater to coat and protect surfaces. mcfp-1/HA coacervates exhibited excellent wear protection on mica with no damage from applied loads, $F_{\perp}$, as high as 300 mN (pressure, P, > 2 MPa).[27,29,32] Recombinant proteins only partially recapitulated the wear protective effect: surfaces with rmfp-1/HA coacervates were damaged under 10-fold lower loads than surfaces with mcfp-1/HA coacervates. Coacervate surface wear protection was independent of the coefficient of friction but dependent on Dopa and polycation to polyanion mixing ratio. The wear protection in mcfp-1/HA coacervates suggests that retention of a fluidic component in the cuticular matrix may substantially contribute to damage mitigation in the mussel byssus.

We began by investigating the conditions under which mfp-1/HA coacervates. We found that the degree of coacervation was dependent on salt concentration, pH, and polyanion/polycation mixing ratio. When combined, mcfp-1 and HA coacervated over a 10-fold range of salt concentrations, over the tested pH range of 3.3−4.5, and across all tested polyelectrolyte mixing ratios. Recombinant rmfp-1, both with and without Dopa, also coacervated with HA but were more easily destabilized by salt than the mcfp-1/HA coacervates (Figure 2b). The greater salt tolerance of mcfp-1/HA coacervates may be due to the difference in molecular weight between the native and recombinant proteins ($MW_{mcfp\text{-}1}$ = 92KDa vs $MW_{rmfp\text{-}1}$ = 14KDa). Nonetheless, both mcfp-1 and rmfp-1 coacervate systems delivered concentrated material underwater. To our knowledge, this is the first report of a complex coacervate made from native mussel foot proteins.

Widespread use of complex coacervates in coating and encapsulation technologies for granules, drugs, and perfumes depends critically on their adhesion/cohesion energy, E_{ad}, and interfacial energy, γ_{eff}.[33] We investigated the adhesion/cohesion energy and the interfacial energy to determine how thoroughly mfp-1/HA coacervates coat surfaces. Coacervates were injected as microdroplets into the SFA and allowed to settle on and coat a mica surface. All tested mfp-1/HA coacervates adhered to mica ($0.42 \pm 0.12 < E_{ad} < 1.08 \pm 0.25$ mJ/m^2) and exhibited low interfacial energy ($0.28 \pm 0.08 < \gamma_{eff} \leq 0.72 \pm 0.17$ mJ/m^2 (Figure 5). mcfp-1/HA coacervate at a 1:1 mixing ratio had the lowest interfacial energy ($\gamma_{eff} = 0.28 \pm 0.08$ mJ/m^2) of all the coacervate systems tested, exhibiting the lowest γ_{eff} ever reported for liquid−liquid separations.[33] Visual investigations confirmed that all tested coacervates efficiently coated the surfaces (Figure 4), making them well suited for coating cuticle granules and encapsulation technologies.

After coating the mica surface with the mfp-1/HA coacervate, we investigated frictional damage mitigation by exposing the coacervate-covered mica surface to shear in the SFA. Here, wear protection is defined as the maximum load, F_D, that coacervate-coated mica surfaces withstood before exhibiting shear-induced damage (Figure 4). mcfp-1/HA coacervate mitigated frictional damage to mica surfaces, even under applied normal loads of 300 mN (pressure, P > 2 MPa). rmfp-1/HA coacervate achieved only a fraction of the wear protective effect; shear induced damage with rmfp-1/HA coacervate under 10-fold lower loads than with mcfp-1/HA coacervate. That coacervated native protein dissipated energy and resisted frictional wear to surfaces suggest that the cuticle matrix plays a crucial role in mitigating shear-induced damage in the byssus (Figure 1).

We did not expect this damage mitigation because all our coacervates exhibited a comparatively high coefficient of friction, (μ = 0.3) (rmfp-151/HA coacervate, μ = 1.3;[24] and synovial fluid, μ = 0.15[28]). However, the coefficient of friction has increasingly been shown to be an invalid measure of surface damage: several studies of lubricants with a low coefficient of friction report poor wear protection to mica surfaces and especially to biological tissues.[27,29,34] Our observation that mfp-1/HA coacervates with the same coefficient of friction (μ = 0.3) vary more than 10-fold in damage mitigation supports the notion that damage mitigation is dependent on more than just the coefficient of friction; we found that damage mitigation correlates to both polyanion-to-polycation mixing ratio and surface adhesion.

Mfps adhere readily to mica surfaces through a combination of bidentate hydrogen bonding of Dopa and electrostatic interactions between positively charged lysine and negatively charged mica.[35] The recombinant protein lacks Dopa that can be added to the protein to demonstrate the effect of surface adhesion to wear protection. In the absence of Dopa, rmfp-1/HA coacervate is unable to remain attached to mica, allowing frictional stresses to act directly on the mica surface, resulting in

DOI: 10.1021/acsbiomaterials.5b00252
ACS Biomater. Sci. Eng. 2015, 1, 1121−1128

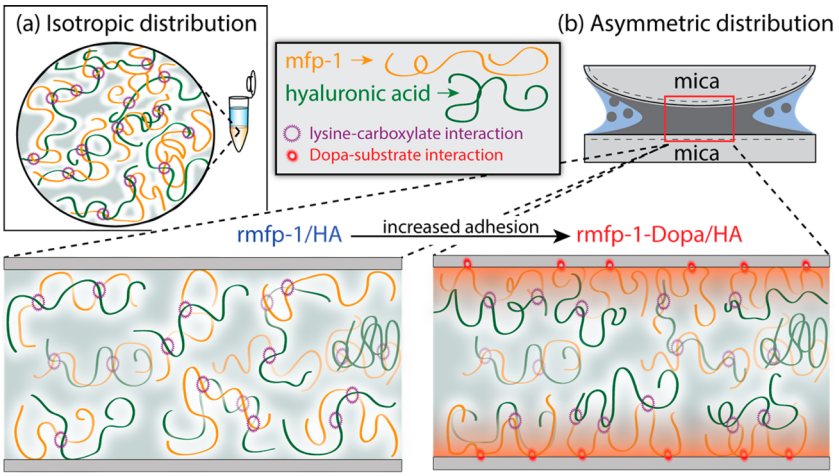

Figure 7. Schematic of the proposed wear protection mechanism. Coacervates, condensed by numerous transient electrostatic interactions between lysine and carboxylate moieties (purple asterisk), (a) isotropically distribute in the bulk solution and (b) distribute asymmetrically under compressive shear with mfp-1 (yellow) preferentiality bound to the surface. Adding Dopa to mfp-1 increases adhesion to mica (red asterisk) and increases wear protection by shifting the slip-plane away from the mica and into the intervening layer enriched with HA (green).

surface damage under low loads (F_D < 10 mN, Figures 6 and 7). Addition of Dopa in rmfp-1 increased surface adhesion and protected the surfaces from damage under 5-fold higher loads (F_D < 60 mN) (Figures 6 and 7). We propose that under compressive shear, mfp-1/HA coacervates with Dopa (rmfp-1-Dopa/HA and mcfp-1/HA) undergo redistribution where Dopa mediates adhesion between mfp-1 and mica. In this way, the surfaces are protected from damage by shifting the slip-plane up from the surface into the intervening coacervate layer, a reconfiguration that has been described as incompressible "molecular ball bearings."[25,36,37]

To further investigate the mcfp-1/HA coacervates, we adjusted the polycation-to-polyanion mixing ratio (7:3 and 3:7) and found that surface wear protection relied on the careful coordination of the mixing ratio. Although mcfp-1/HA coacervates at a 1:1 mixing ratio protected the surfaces from damage at high loads, mcfp-1/HA coacervated at suboptimal 7:3 and 3:7 mixing ratios weakly protected surfaces, which were damaged under only a quarter of the applied load (Figures 4a and 5). In this instance, damage was not due to insufficient adhesion; mcfp-1/HA coacervates with an excess of mcfp-1 or HA had higher adhesion/cohesion energies. Perhaps these molecules not involved in balanced electrostatic interactions (coacervate formation) become entangled, allowing shear forces to impact and damage the surface. The observation that as adhesion increases, wear protection also increases up to a point suggests that adhesion has an optimum for mitigating damage.

Mussel byssal cuticle toughness and durability is widely attributed to covalent cross-links and Ca^{2+} and Fe^{3+} complexation.[16,38] However, our results raise the interesting possibility that maintaining coacervates (fluid components), perhaps stabilized by microenvironments[39] in the cuticle matrix, could be adaptively beneficial for damage control as well as self-healing since fluids spontaneously self-heal. The excellent frictional damage mitigation by mcfp-1/HA coacervates reveals a significant untapped potential for coacervates in applications that require both adhesion and energy-dissipative lubrication, such as artificial joints, contact lenses, dental sealants, and hair and skin conditioners.

4. CONCLUSIONS

We delivered mussel cuticle matrix-inspired blends in a concentrated form underwater as complex coacervates. They coated surfaces, dissipated energy, and protected surfaces from wear. Damage mitigation was independent of the coefficient of friction and dependent on surface adhesion and coacervation conditions. On the basis of these results, we propose that during compressive shear, coacervated mfp-1 and HA undergo redistribution whereby Dopa mediates adhesion between mfp-1 and mica. The adhesive layer protects the mica surface by shifting the slip-plane up from the surface into the intervening coacervate layer. mcfp-1/HA coacervates exhibited exceptional surface damage mitigation against shear-induced wear, suggesting that retention of a fluidic component in the cuticular matrix may substantially contribute to damage mitigation in the mussel byssus.

5. MATERIALS AND METHODS

5.1. Purification of Native mcfp-1. We purified native mcfp-1 as described previously,[40] with some modifications. We harvested mussels from the pilings of Goleta Pier (Santa Barbara, CA) and held them in circulation tanks. The mussels were shucked, and their feet were amputated and stored at −70 °C before flaying off the pigmented epithelium. Approximately 50 prepared feet were homogenized in four equivalents (w/v) of 5% acetic acid (v/v), 10 μM leupeptin, 10 μM pepstatin, and 1 mM ethylenediaminetetraacetic acid in a glass Kontes tissue grinder (Vineland, NJ) on ice, then centrifuged at 20,000g and 4 °C for 40 min. The supernatant was acidified to 1.5% (v/v) perchloric acid. After centrifugation at 20,000g and 4 °C for 40 min, the supernatant was dialyzed for four rounds in 4 L of 5% acetic acid (v/v) for 4 h (1000 Da molecular weight cutoff tubing from Spectrum Industries, Los Angeles, CA) before lyophilization. Lyophilized protein was resuspended in 200 μL of 5% acetic acid (v/v), and 50 μL aliquots were run through a Shodex KW-803 size exclusion column (5 μm, 8 × 300 mm) (Showa Denko, New York, NY). Fractions were monitored at 280 nm, and those that absorbed were assessed for sample purity by acid-urea polyacrylamide gel electrophoresis [7.5% acrylamide, 0.2% *N*,*N*-methylenebis-(acrylamide), 5% acetic acid, and 8 M urea gels then stained with Coomassie Blue R-250 (Sigma-Aldrich, Brooklyn, NY)] and amino acid analysis. Pure mcfp-1 fractions were pooled and aliquoted before lyophilization and stored at −70 °C for future use.

5.2. Recombinant mfp-1 (rmfp-1) and Enzymatic Modification of rmfp-1 Tyrosine to Dopa. rmfp-1 was prepared as in Zheng

DOI: 10.1021/acsbiomaterials.5b00252
ACS Biomater. Sci. Eng. 2015, 1, 1121−1128

et al.[41] and was provided by D.S. Hwang (Pohang University of Science and Technology University, Pohang, S. Korea). rmfp-1 consisted of the sequence $[AKPSYPPTYK]_{12}$ (with a point mutation Ser_{65} to Cys_{65}). The decapeptide repeat sequence of rmfp-1 is the same as that of the *M. californianus* decapeptide repeat sequence except that the first three positions in the recombinant repeat sequence (AKP*) correspond to the repetitive sequence found in *M. galloprovincialis*, which varies slightly from that of the *M. californianus* repeat (P*KI). Proteins having extensive internal repeat sequences are not well tolerated by *Escherichia coli*, hence the use of less than full-length versions here (MW_{rmfp-1} = 14KDa vs MW_{mfp-1} = 92KDa). Recombinant mfp-1 also has a lower molar Dopa content (~18 vs 92 Dopa residues, respectively) and lacks post-translational hydroxylation of prolines seen in mcfp-1.

Tyrosine (Tyr) to Dopa enzymatic modification was done as before,[42] with some modifications. rmfp-1 (1 mg) was dissolved in 1 mL of pH 7, 10 mM borate and 50 mM phosphate-ascorbate buffer. After adding mushroom tyrosinase (0.3 mg, 3000 U/mg, Sigma-Aldrich), the solution was shaken for 4 h at ambient room temperature and pressure. The reaction was stopped by adding 40 μL of glacial acetic acid and then run through a reverse phase high performance liquid chromatography column and eluted with a linear gradient of acetonitrile. The eluent was monitored continuously at 230 and 280 nm, and fractions containing protein were pooled and lyophilized. Amino acid analysis of the final product indicated a Tyr to Dopa conversion of ~83% in rmfp-1 (further referred to as rmfp-1-Dopa).

5.3. Coacervation of mfp-1 and HA: Effects of Ionic Strength, pH, and Mixing Ratio. We quantified coacervate yield under different solution conditions via turbidimetric measurements. Each solution was prepared by dissolving either mfp-1 or HA (0.3 mg/mL) in sodium acetate buffer [10 mM at pH 3.7 or 4.7 and either 10 mM NaCl (rmfp-1 and rmfp-1-Dopa) or 60 mM NaCl (mcfp-1)]. Because maximum coacervation occurs with polymers of matching molecular weights,[43] rmfp-1 (14 kDa) was matched with a 35 kDa version of HA, and mcfp-1 (92 kDa) was matched with a 76 kDa HA (Lifecore Biomedical, Chaska, MN).

For mixing ratio measurements, we added HA (0.3 mg/mL) to a mfp-1 solution (0.3 mg/mL) at varying volume ratios in sodium acetate/acetic acid buffer (pH 3.7). We investigated ionic strength dependence by adjusting the NaCl concentration at a 1:1 weight ratio of mfp-1 to HA (calculated charge ratio of 0.71:1 polycation to polyanion for both mcfp-1/HA and rmfp-1/HA coacervates using Lys pK_a= 10.5 and HA-COOH pK_a= 2.9[44]) in sodium acetate/acetic acid buffer (pH 3.7).

5.4. Microscopic Confirmation of the Coacervate Phase. We mixed mfp-1 and HA just prior to their injection (<1 min) between a glass slide and coverslip separated by double-sided tape. Light microscope images were taken with a Zeiss Axioplan microscope equipped with an optronics macrofile CCD camera at 100× magnification 10 min postinjection to monitor coacervate formation.

5.5. Measuring Normal and Lateral Interactions. We measured the normal and lateral forces as a function of the separation distance, D, between surfaces using the SFA as before[24,45,46] with some modifications. Mica was used because it provides a sensitive testing ground for frictionally induced damage as it is unable to endure shear stresses and therefore shows shear-induced damage under low loads ($F_\perp$ < 10 mN).[47] We prepared mica surfaces by manually cleaving mica and then gluing a thin, freshly cleaved mica sheet (1−5 μm) onto a cylindrical silica disk ($R \approx 2$ cm) with thermoset epoxy resin (Epon 1004F). The two curved mica surfaces were mounted in the SFA in a crossed-cylinder geometry, which roughly corresponds to a sphere of radius R on a flat surface based on the Derjaguin approximation. The bottom surface was supported by a double cantilever spring from which the normal forces were measured and connected to a piezoelectric bimorph slider for shear measurements. Mica−mica separation distances (D) were measured by multiple beam interferometry[48] with Å level distance resolution by first measuring the mica−mica contact distance, D = 0, in air and using it as a reference distance for all other measurements.

We mixed mfp-1 (0.3 mg/mL) and HA (0.3 mg/mL) less than 1 min prior to injecting 50−100 μL of the mixture between the two mica surfaces in the SFA where the mfp-1/HA coacervate coalesced, settled on, and coated the mica surface (30 min, Figure 4). Alternatively, coacervates may be premixed and used in their dense phase; however, this increases time requirements and results in material loss. The force of adhesion (F_{ad}) was used to calculate the interfacial energy ($\gamma_{eff} = F_{ad}/3\pi R$) [the energy required for a coacervate and create new, solvent (equilibrium phase) exposed surface][33] and the interaction (adhesion/cohesion) energy (by the Derjaguin approximation, $W_{ad} = F_{ad}/2\pi R$).

We sheared the surfaces at a sliding velocity of 10−100 μm/s with a friction device.[45] The coefficient of friction (μ) is defined as the slope of $F_{||}$ versus $F_\perp$ plot. Aberrations in the FECO and Newton rings indicated damage to the mica surface (Figure 4). The SFA allows for verification of a continuous coacervate coating. For every experiment, we confirmed a continuous coacervate coating of the surface through continuity of the FECO and measured the normal and lateral forces without sample disruption. All SFA experiments were performed at room temperature (thermostated at 23 °C).

AUTHOR INFORMATION

Corresponding Author

*Phone: +1 805-893-2817. E-mail: waite@lifesci.ucsb.edu.

Notes

The content of the information does not necessarily reflect the position or the policy of the government and no official endorsement should be inferred.

The authors declare no competing financial interest.

ACKNOWLEDGMENTS

This research was supported by grants from NIH (R01 DE18468) and the Institute for Collaborative Technologies through grant W911NF-09-0001 from the US army research office. This work was partially supported by the MRSEC Program of the National Science Foundation under Award No. DMR 1121053. We thank Dong Soo Hwang of POSTECH for the gift of recombinant mfp-1, Danny DeMartini for the cuticle micrograph, Claus Eisenbach for fruitful discussions on polymer dynamics, Maryte Gylys for her assistance in protein purification and turbidimetric analysis, and Wei Wei for her assistance in rmfp-1 enzymatic modification.

REFERENCES

(1) Denny, M. W.; Miller, L. P.; Stokes, M. D.; Hunt, L. J. H.; Helmuth, B. S. T. Extreme water velocities: topographical amplification of wave-induced flow in the surf zone of rocky shores. *Limnol. Oceanogr.* **2003**, *48*, 1−8.

(2) Carrington, E.; Gosline, J. M. Mechanical design of mussel byssus: load cycle and strain rate dependence. *Am. Malacol. Bull.* **2006**, *18*, 135−142.

(3) Park, J. Y.; Salmeron, M. Fundamental Aspects of Energy Dissipation in Friction. *Chem. Rev.* **2014**, *114*, 677−711.

(4) Begley, M. R.; Collino, R. R.; Israelachvili, J. N.; McMeeking, R. M. Peeling of a tape with large deformations and frictional sliding. *J. Mech. Phys. Solids* **2013**, *61*, 1265−1279.

(5) Danner, E. W.; Kan, Y.; Hammer, M. U.; Israelachvili, J. N.; Waite, J. H. Adhesion of mussel foot protein mefp-5 to mica: an underwater superglue. *Biochemistry* **2012**, *51*, 6511−6518.

(6) Israelachvili, J. N.; Chen, Y.-L.; Yoshizawa, H. Relationship between adhesion and friction forces. *J. Adhes. Sci. Technol.* **1994**, *8*, 1231−1249.

(7) Bell, E. C.; Gosline, J. M. Strategies for life in flow: Tenacity, morphometry, and probability of dislodgment of two Mytilus species. *Mar. Ecol.: Prog. Ser.* **1997**, *159*, 197−208.

DOI: 10.1021/acsbiomaterials.5b00252
ACS Biomater. Sci. Eng. 2015, 1, 1121−1128

(8) Qin, Z.; Buehler, M. J. Impact tolerance in mussel thread networks by heterogeneous material distribution. *Nat. Commun.* **2013**, *4*, article # 2187 10.1038/ncomms3187
(9) del Campo, A.; Greiner, C.; Arzt, E. Contact Shape Controls Adhesion of Bioinspired Fibrillar Surfaces. *Langmuir* **2007**, *23*, 10235−10243.
(10) Bertoldi, K.; Boyce, M. C. Mechanics of the hysteretic large strain behavior of mussel byssus threads. *J. Mater. Sci.* **2007**, *42*, 8943−8956.
(11) Waite, J. H.; Qin, X.-X.; Coyne, K. J. The peculiar collagens of mussel byssus. *Matrix Biol.* **1998**, *17*, 93−106.
(12) Harrington, M. J.; Waite, J. H. Holdfast heroics: comparing the molecular and mechanical properties of Mytilus californianus byssal threads. *J. Exp. Biol.* **2007**, *210*, 4307−4318.
(13) Holten-Andersen, N.; Zhao, H.; Waite, J. H. Stiff coatings on compliant biofibers: the cuticle of Mytilus californianus byssal threads. *Biochemistry* **2009**, *48*, 2752−2759.
(14) Holten-Andersen, N.; Fantner, G. E.; Hohlbauch, S.; Waite, J. H.; Zok, F. W. Protective coatings on extensible biofibres. *Nat. Mater.* **2007**, *6*, 669−672.
(15) Holten-Andersen, N.; Waite, J. H. Mussel-designed protective coatings for compliant substrates. *J. Dent. Res.* **2008**, *87*, 701−709.
(16) Harrington, M. J.; Masic, A.; Holten-Andersen, N.; Waite, J. H.; Fratzl, P. Iron-clad fibers: a metal-based biological strategy for hard flexible coatings. *Science* **2010**, *328*, 216−220.
(17) Taylor, S. W.; Waite, J. H.; Ross, M. M.; Shabanowitz, J.; Hunt, D. F. Trans-2,3-cis-3,4-Dihydroxyproline, a new naturally occurring amino acid, is the sixth residue in the tandemly repeated consensus decapeptides of an adhesive protein from Mytilus edulis. *J. Am. Chem. Soc.* **1994**, *116*, 10803−10804.
(18) Waite, J. H.; Housley, T. J.; Tanzer, M. L. Peptide repeats in a mussel glue protein: theme and variations. *Biochemistry* **1985**, *24*, 5010−5014.
(19) Vitellaro Zuccarello, L. Ultrastructural and cytochemical study on the enzyme gland of the foot of a mollusc. *Tissue Cell* **1981**, *13*, 701−713.
(20) Stewart, R. J.; Weaver, J. C.; Morse, D. E.; Waite, J. H. The tube cement of Phragmatopoma californica: a solid foam. *J. Exp. Biol.* **2004**, *207*, 4727−4734.
(21) Stewart, R. J.; Wang, C. S.; Shao, H. Complex coacervates as a foundation for synthetic underwater adhesives. *Adv. Colloid Interface Sci.* **2011**, *167*, 85−93.
(22) Kizilay, E.; Kayitmazer, A. B.; Dubin, P. L. Complexation and coacervation of polyelectrolytes with oppositely charged colloids. *Adv. Colloid Interface Sci.* **2011**, *167*, 24−37.
(23) Hwang, D. S.; Waite, J. H.; Tirrell, M. Promotion of osteoblast proliferation on complex coacervation-based hyaluronic acid - recombinant mussel adhesive protein coatings on titanium. *Biomaterials* **2010**, *31*, 1080−1084.
(24) Hwang, D. S.; et al. Viscosity and interfacial properties in a mussel-inspired adhesive coacervate. *Soft Matter* **2010**, *6*, 3232−3236.
(25) Klein, J. Molecular mechanisms of synovial joint lubrication. *Proc. Inst. Mech. Eng., Part J* **2006**, *220*, 691−710.
(26) Kayitmazer, A. B.; Seeman, D.; Minsky, B. B.; Dubin, P. L.; Xu, Y. Protein-polyelectrolyte interactions. *Soft Matter* **2013**, *9*, 2553−2583.
(27) Das, S.; et al. Synergistic interactions between grafted hyaluronic acid and lubricin provide enhanced wear protection and lubrication. *Biomacromolecules* **2013**, *14*, 1669−1677.
(28) Banquy, X.; Lee, D. W.; Das, S.; Hogan, J.; Israelachvili, J. N. Shear-Induced Aggregation of Mammalian Synovial Fluid Components under Boundary Lubrication Conditions. *Adv. Funct. Mater.* **2014**, *24*, 3152−3161.
(29) Yu, J.; Banquy, X.; Greene, G. W.; Lowrey, D. D.; Israelachvili, J. N. The Boundary Lubrication of Chemically Grafted and Cross-Linked Hyaluronic Acid in Phosphate Buffered Saline and Lipid Solutions Measured by the Surface Forces Apparatus. *Langmuir* **2012**, *28*, 2244−2250.
(30) Autumn, K.; Dittmore, A.; Santos, D.; Spenko, M.; Cutkosky, M. Frictional adhesion: a new angle on gecko attachment. *J. Exp. Biol.* **2006**, *209*, 3569−3579.
(31) Das, S.; et al. JKR Theory for the Stick−Slip Peeling and Adhesion Hysteresis of Gecko Mimetic Patterned Surfaces with a Smooth Glass Surface. *Langmuir* **2013**, *29*, 15006−15012.
(32) Forster, H.; Fisher, J. The influence of continuous sliding and subsequent surface wear on the friction of articular cartilage. *Proc. Inst. Mech. Eng., Part H* **1999**, *213*, 329−345.
(33) Priftis, D.; Farina, R.; Tirrell, M. Interfacial energy of polypeptide complex coacervates measured via capillary adhesion. *Langmuir* **2012**, *28*, 8721−8729.
(34) Homola, A. M.; Israelachvili, J. N.; McGuiggan, P. M.; Gee, M. L. Fundamental experimental studies in tribology: The transition from 'interfacial' friction of undamaged molecularly smooth surfaces to 'normal' friction with wear. *Wear* **1990**, *136*, 65−83.
(35) Lu, Q.; Hwang, D. S.; Liu, Y.; Zeng, H. Molecular interactions of mussel protective coating protein, mcfp-1, from Mytilus californianus. *Biomaterials* **2012**, *33*, 1903−1911.
(36) Liberatore, M. W.; Wyatt, N. B.; Henry, M.; Dubin, P. L.; Foun, E. Shear-Induced Phase Separation in Polyelectrolyte/Mixed Micelle Coacervates. *Langmuir* **2009**, *25*, 13376−13383.
(37) Dubin, P. L.; Li, Y.; Jaeger, W. Mesophase Separation in Polyelectrolyte-Mixed Micelle Coacervates. *Langmuir* **2008**, *24*, 4544−4549.
(38) Holten-Andersen, N.; et al. Metals and the integrity of a biological coating: the cuticle of mussel byssus. *Langmuir* **2009**, *25*, 3323−3326.
(39) Longo, G. S.; Olvera de La Cruz, M.; Szleifer, I. Molecular theory of weak polyelectrolyte gels: the role of pH and salt concentration. *Macromolecules* **2011**, *44*, 147−158.
(40) Zhao, H.; Waite, J. H. Linking Adhesive and Structural Proteins in the Attachment Plaque of Mytilus californianus. *J. Biol. Chem.* **2006**, *281*, 26150−26158.
(41) Zeng, H.; Hwang, D. S.; Israelachvili, J. N.; Waite, J. H. Strong reversible Fe3+-mediated bridging between dopa-containing protein films in water. *Proc. Natl. Acad. Sci. U. S. A.* **2010**, *107*, 12850−12853.
(42) Taylor, S. W. Chemoenzymatic Synthesis of Peptidyl 3,4-Dihydroxyphenylalanine for Structure−Activity Relationships in Marine Invertebrate Polypeptides. *Anal. Biochem.* **2002**, *302*, 70−74.
(43) Chollakup, R.; Beck, J. B.; Dirnberger, K.; Tirrell, M.; Eisenbach, C. D. Polyelectrolyte molecular weight and salt effects on the phase behavior and coacervation of aqueous solutions of poly(acrylic acid) sodium salt and poly(allylamine) hydrochloride. *Macromolecules* **2013**, *46*, 2376−2390.
(44) Reed, C. E.; Li, X.; Reed, W. F. The effects of pH on hyaluronate as observed by light scattering. *Biopolymers* **1989**, *28*, 1981−2000.
(45) Luengo, G.; Schmitt, F.-J.; Hill, R.; Israelachvili, J. Thin film rheology and tribology of confined polymer melts: contrasts with bulk properties. *Macromolecules* **1997**, *30*, 2482−2494.
(46) Zeng, H.; Tian, Y.; Zhao, B.; Tirrell, M.; Israelachvili, J. Friction at the Liquid/Liquid Interface of Two Immiscible Polymer Films. *Langmuir* **2009**, *25*, 4954−4964.
(47) Liu, Y.; Wu, T.; Evans, D. F. Lateral Force Microscopy Study on the Shear Properties of Self-Assembled Monolayers of Dialkylammonium Surfactant on Mica. *Langmuir* **1994**, *10*, 2241−2245.
(48) Israelachvili, J.; et al. Recent advances in the surface forces apparatus (SFA) technique. *Rep. Prog. Phys.* **2010**, *73*, 036601.

DOI: 10.1021/acsbiomaterials.5b00252
ACS Biomater. Sci. Eng. 2015, 1, 1121−1128